High-power and low-intensity noise laser at 1064nm

Germain Guiraud, Nicholas Traynor, Giorgio Santarelli

High power and low intensity noise laser at 1064nm

GERMAIN GUIRAUD, [1, 2,*] NICHOLAS TRAYNOR, [1] GIORGIO SANTARELLI, [2]

[1] Azur Light Systems, Av. de la Canteranne, Pessac, France
[2] Laboratoire Photonique, Numérique et Nanosciences, CNRS, Université de Bordeaux, Institut d'Optique, Talence, France
*Corresponding author: gguiraud@azurlight-systems.com

We have developed a single-frequency, narrow linewidth (Δν<50 kHz) laser operating at 1064nm with high output power (50W). This laser is based on an Ytterbium doped fiber master oscillator power amplifier architecture with output beam at diffraction limit. An output power of 50W is obtained with two amplification stages using a 50mW diode laser seeder. We have carefully studied the relative intensity noise at each amplification stage. The detrimental effect due to Stimulated Brillouin Scattering on residual amplitude noise has been observed on the high power booster stage. After careful optimization this laser exhibits low intensity noise with a RMS value equal to 0.012% [1 kHz/10MHz]@50W.

High power fiber lasers are widely used in several domains as fundamental physics and semiconductor industry. Fiber laser technology offers several advantages: broad gain window (1020 – 1090nm for Yb), power scaling with high wall-plug efficiency, good beam quality and pointing stability [1, 2]. Low noise single frequency operation is mandatory for demanding physics experiments such as cold atom optical lattices, frequency metrology and gravitational wave detectors [3].

Single frequency high power MOPA fiber lasers have already been demonstrated by several groups [4, 5]. Despite the impressive advances in these high power lasers, the relative intensity noise has not been fully investigated.

In this letter, we report on the development of an industrial grade low intensity noise laser operating at 1064nm with an output power of 50W.

In single frequency and high power regimes, several noise sources can impair low noise operation, like amplified spontaneous emission (ASE), Brillouin and Rayleigh scattering [6,7].

During this development, we have investigated and optimized the intensity noise of each part of this laser. In particular, we have highlighted the effect of SBS. In addition, during this study, we have taken into account the constraints of an industrial solution. For instance, we focus on all-fiber architecture, robust, cost effective and free of any active noise reduction system.

This MOPA Ytterbium doped fiber laser is composed of two amplification stages, seeded by a low noise, low power (50mW) single frequency laser diode. Single stage amplification from tens of mW up to tens of watts is impractical and can potentially lead to unstable operation.The preamplifier generates more than 1W whereas the main amplifier allows us to reach 50W at 1064 nm with a slope efficiency approaching 80%. Both amplifiers are cladding pumped with grating stabilized multimode pump diodes at 976nm. Figure 1 shows this schematic of the laser.

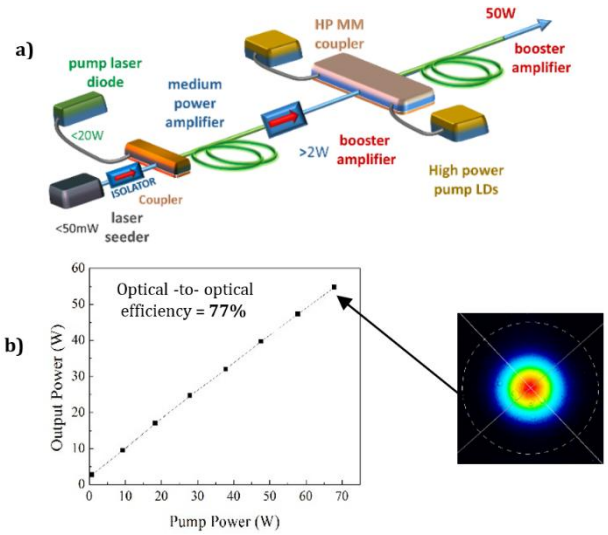

Fig. 1. a) Schematic of high power single frequency MOPA laser. b) Optical-to-optical efficiency (on the left) and beam profile at 50W (on the right)

In order to carefully study and optimize each element of the laser to minimize the relative intensity noise, we developed a custom low noise photodetector. This device is able to handle up to 20 mW of optical power while exhibiting a noise floor lower than –170 dBc/Hz from 1 kHz to 10 MHz when the incident optical power is 10 mW. By measuring the intensity noise power spectral density using a Fast Fourier Transform (FFT) analyzer, we have been able to identify different noise sources in the frequency domain from 1 kHz to 10MHz. For instance, technical noise from electrical supplies and acoustics are generally confined below 10 kHz. Pump laser noise can affect the spectrum up to 100 kHz as we show below. Beyond 100 kHz, where the impact of technical noise is strongly reduced, the dominant effects are related to more fundamental effects as shot noise, amplified spontaneous emission or SBS.

In order to study the intensity noise, we need a very low noise laser seeder. As we focus on single frequency operation at 1064 nm, we have the choice among several technologies: NPRO laser (Non Planar Ring Oscillator), fiber Bragg grating laser or laser diodes (DBR (Distributed Bragg Reflector), DFB (Distributed Feedback) or ECDL (Extended Cavity Diode Laser)).

The NPRO laser shows both very low intensity noise and narrow linewidth. However, the factor form, the cost and the lack of integrated fiber pigtail reduce the interest for an industrial

application. Fiber laser are robust and narrow linewidth but shows a significant level of intensity noise [8, 9].

Laser diodes are a very appealing alternative to previous solutions. For instance, packaging technologies allow very compact and robust fiber pigtailed devices. It is well known that laser diodes RIN is potentially very low. The linewidth ranges from MHz or less for DBR and DFB devices downs to tens of kHz for ECDL.

We choose a fiber pigtailed device without integrated isolator which potentially delivers hundreds of mW of optical power. A significant effort has been deployed on thermo-mechanical packaging and optical isolation for improved wavelength stability and stable low noise operation. We have investigated two commercially available laser diodes: an ECDL and a DBR. The linewidth of each laser diode has been measured by beatnote techniques respect to a narrow fiber laser showing well below 30 kHz for ECDL (see figure 2 for the frequency noise power spectral density (PSD) of the ECDL seeder) and about 1 MHz for DBR (not shown here). The ECDL can deliver in excess of 300 mW while the DBR is limited to about 50 mW.

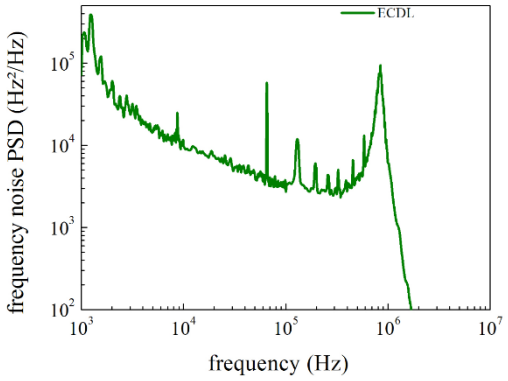

Fig. 2. Frequency noise power spectral density (PSD) of ECDL seeder at 1064nm. Beyond 500 kHz, measurement artefacts are dominant.

We have measured the intensity noise for both devices after careful optimization of the current driver noise and minimized the optical feedback, which has been showed to be detrimental.

In figure 3, we show the measured RIN spectral densities. Both laser shows a very low intensity noise approaching -160 dBc beyond few hundred kHz. The ECDL shows an overall better intensity noise especially at low Fourier frequencies. For this reason, we choose this laser diode for seeding our Ytterbium MOPA fiber laser. The ECDL and DFB based seed lasers are fully functional laser modules produced by Azur Light Systems.

Single stage amplification from tens of mW up to tens of watts is impractical and can potentially lead to unstable operation. It's thus interesting to investigate the noise properties of amplifiers with output powers ranging from half a watt to a few watts. We experimented different ways to develop the lower intensity noise preamplifier.

In this next part, we will discuss both pumping method (namely core and clad pumping schemes) and intensity noise of different commercial doped fibers (here, 5/130µm and 10/125µm).

The intensity noise dynamic due to pump-to-signal coupling and the input to output transfer function in low power Yb MOPA fiber in the sub watt regime has been already developed and studied in previous works [10, 11, and 12].

In the case of low residual pump power and moderate to high gain, the pump-to-signal noise transfer function can be modeled by a low-pass filter with cut-off frequency given by:

$$\omega_{eff} \approx P_s^0(L).B_s \qquad (1)$$

where $P_s^0(L)$ is the average signal power at the end of the fiber given in number of photons per second. The coupling factor B_s depends on the signal overlap with the doped region Γ_s, the signal cross section for signal absorption and emission σ_{12}, σ_{21} and the fiber mode field area A (~a few 10^{-11}m²).

$$B_s = \Gamma_s(\sigma_{12} + \sigma_{21})/A \qquad (2)$$

It can be seen that the corner frequency is proportional to the amplifier output power. Thus when the seeder has very low noise as in our case the Fourier frequency range below ω_{eff} is fully dominated by the pump intensity noise.

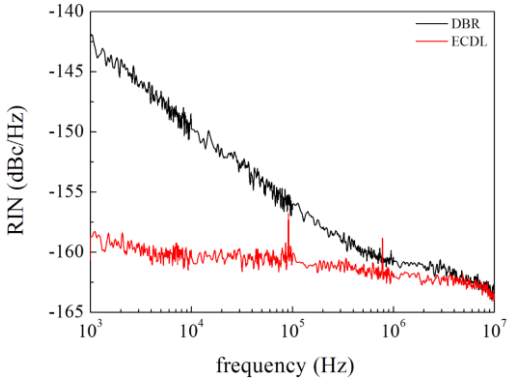

Fig. 3. Relative Intensity Noise of both DBR and ECDL seeder diode

With core pumping in YDF, we can reach very good efficiency (near 90%).

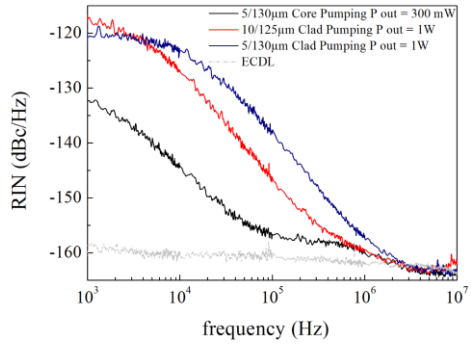

Fig. 4. Comparison of core pumping and clad pumping intensity noise in Ytterbium doped fiber

The clad pumping approach is slightly less efficient but allows the generation of larger optical power by using high power multimode pumping.

The RIN measurement results of the core and clad pumping amplifiers are given in figure 4.

For core pumping, we use a single spatial mode laser diode which shows very low intensity noise compared to multimode

diode pumps in clad pumping. Each laser pump operates at 976nm, the Ytterbium absorption peak.

We observe that core pumped configuration shows better RIN level due both to single mode diodes noise and to a lower ω_{eff} due to the lower output power. However, in the case of high output power amplifier (>10W) we need to seed with a power in excess of 1W. We thus investigated a preamplifier stage able to increase the optical power from tens of mW up to a few Watts.

We can observe that the amplification process adds excess noise compared to ECDL seed noise between 1 kHz and 100 kHz for core pumping and between 1 kHz and 700 kHz for clad pumping.

The low seeder noise is recovered at higher frequencies.

Even if core pumping shows the lowest noise configuration, we implement the clad pumping technique for our preamplifier allowing in excess of 4W output power.

In figure 4 and with the analytical model seen above, we can observe two mains contributions of ω_{eff} in fiber amplifiers: core area (in cm^2) and optical output power. A larger core fiber area leads to a reduction of corner frequency whereas an increase of output power has the inverse contribution. In our case, for the same output power (1W), with 5/130 and 10/125µm Yb doped fibers, we can observe that the corner frequency is lower for the larger fiber as expected. With 10/125µm fiber, a level of -150 dBc/Hz is reaching at 200 kHz against 400 kHz for a 5/130µm fiber.

From equation [1] and |2], we can estimate the corner frequency for each fiber type, provided that all fiber parameters are well defined, in particular signal cross section for absorption and emission (σ_{12} and σ_{21}) and the signal overlap with the doped region Γ. The cross sections mainly depend on the host material: aluminosilicate, phosphosilicate or a combination of the two. The overlap can be easily calculated with the following equation:

$$\Gamma = 1 - exp\,(2 - \frac{r_{co}^2}{w^2}) \qquad (3)$$

where $r_{co}$is the core radius of the fiber and w is mode field radius. In our case, $\Gamma_{10/125}$=0.8 and $\Gamma_{5/135}$=0.62.

In the paper of Zervas et al, absorption and emission cross section for aluminosilicate and phosphosilicate host material are reported [13]. In this paper, we can see that phosphosilicate glasses show both absorption and emission cross section reduction compared to aluminosilicate glasses leading to a higher dopant concentration without significant clustering effects. These properties allow the reduction of photo-darkening, one of the most important problem for high power fiber lasers. From this paper, we can estimate signal cross section for emission at 1064nm: $1.3\ 10^{-25} m^2$for phosphosilicate and $4.2\ 10^{-25} m^2$ for aluminosilicate.

We expect that for the 5/130µm Yb-doped fiber, which is used mainly in low power applications, the host material is aluminosilicate. The signal cross section emission for this fiber is estimated to $4.2\ 10^{-25}$m².

For the 10/125µm fiber, Zhang et al [14] report a value of $2.5\ 10^{-25}$m². In fact, phosphorus is incorporated in an aluminosilicate host material in order to reduce photo-darkening effect. In our calculation assume an average cross-section of $2.75\ 10^{-25}$m² with an error bar of about 50%.

Using these parameters, we compare experimental and theoretical values of corner frequency for these fibers. The experimental determination of the corner frequency is also affected by a measurement error bar of about 30%.

This comparison is shown in table 1.

	5/130	10/125
φ_{core} (µm)	5	10.7
Area (m^2)	$2\ 10^{-11}$	$9\ 10^{-11}$
signal cross section for absorption σ_{12} (m^2)	negligible (10^{-27})	negligible (10^{-27})
signal cross section for emission σ_{21} (m^2)	$4.2\ 10^{-25}$	$2.75\ 10^{-25}$
overlap with the doped region Γ	0.62	0.8
theoretical corner frequency (kHz)	13.2	2.6±1.6
experimental corner frequency (kHz)	15.8±5	3.7±1

Table. 1. Comparison of theoretical and experimental corner frequency for 5µm and 10µm fiber

The comparison of experimental and theoretical values agrees well within the error bars.

The booster amplification stage is composed of a multimode pump combiner and two 60W pump diodes at 976nm.

The MOPA configuration shows an output optical power of 50W at 1064 nm with a launched pump power of 65W corresponding to an optical-to-optical efficiency of 75 %, with a M^2<1.1 a PER >20dB and signal to ASE ratio of over 55 dB (0,07nm resolution bandwidth). This main amplification stage is a homemade all-fiber amplifier module with 17 µm mode field diameter. The fiber length is 3.5m.

In the high power regime, with doped fibers as gain medium, we can observe nonlinear effects such as Raman or Brillouin scattering. The intensity coupling mechanisms between Stoke and pump waves have been investigated in telecom fiber amplifier and Brillouin lasers. In our case the situation is slightly more complex due to the Ytterbium doped fiber gain mechanism.

Several approaches have applied to mitigate the SBS in high power amplifiers. For instance, strain and temperature gradients have been successfully applied to lower SBS threshold [14, 15]. Moving to large mode area fibers is also a possible alternative, but fusion splicing of such fibers requires highly specialized equipment and mode quality is difficult to maintain.

The aim of this MOPA development is to deliver an industrial grade laser system which avoids using rather sophisticated SBS mitigation schemes. We thus focus the optimization of fiber length and seed optical power to minimize the excess RIN in our system.

In figure 5, we show the RIN of this MOPA system. For clarity, we report the output noise of the preamplifier and the typical pump RIN. We can observe that RIN at low frequency is dominated by the technical noise of the pump diodes. The RIN PSD decreases from -120 dBc to -125 dBc when output power is

scaled from 25 to 50W. This reduction originates both from pump noise reduction at higher current operation and gain saturation in the gain medium. At high frequency (> 1 MHz), the noise spectral density rolls down close to the preamplifier noise level. This behavior is qualitatively similar to that already highlighted in the preamplifier. The few dB of excess noise at 50W output are due to the SBS effect.

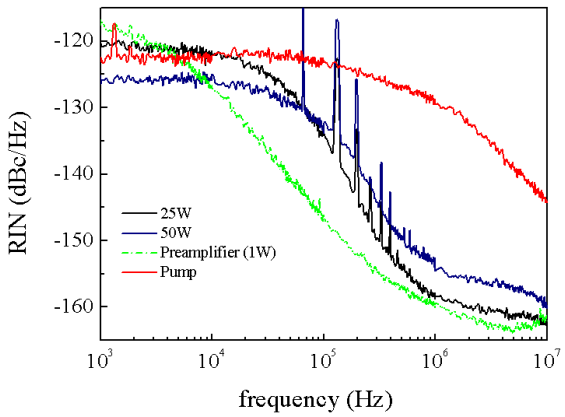

Fig. 5. Relative Intensity Noise [1 kHz-10 MHz] of the YDF MOPA laser in various power output regimes (input power 1W).

Following the work of Horowitz et al [16], we implemented qualitative broad-band RIN measurements ([1-200 MHz]) to detect the spectral signature of SBS. Beyond 50W we observe a steep noise increase with output power up to 150 MHz. The spurious lines around several hundreds of kHz due to power supplies can be easily filtered. The very low RIN Power Spectral Density (PSD) is reproducible to better than 2 dB on the MOPA systems produced at industrial level (several tens of systems). The spurious lines around several hundreds of kHz due to power supplies can be easily filtered. The very low RIN Power Spectral Density (PSD) is reproducible on the MOPA systems produced at industrial level. Furthermore, for industrial applications, a long term power stability test over 8h is carried out.

We obtain a power stability fluctuation of about 1.2% (peak-to-peak) without using any electronic power control feedback during 8h, as we can see in figure 6.

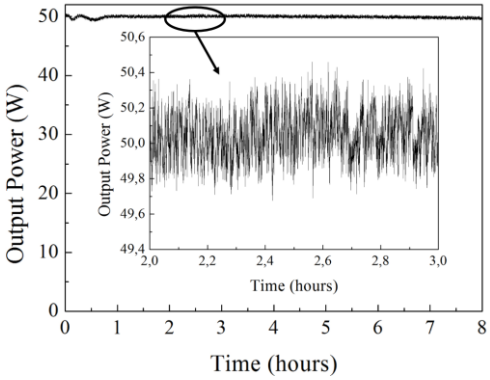

Fig. 6. Long term power stability of the YDF MOPA laser during 8 hours

We demonstrate an all-fiber, high power, low intensity noise Ytterbium MOPA fiber laser with more than 50W output power. By choosing a low noise laser seeder we have been able to optimize each amplifier stage. We also been able to reduce the detrimental effect of the SBS in the booster stage by optimizing the input power and fiber length. At 50W output power this industrial grade laser shows an RIN RMS value equals to 0.012% [1 kHz-10MHz]. In addition, the low RIN at high Fourier frequency (<150dBc@1MHz) enables the implementation of a wideband noise eater. In the future we plan to develop a 100W class ultra-low RIN laser using LMA fibers.

Funding. ANR 14 LAB05 0002 01 and Conseil Regional d'Aquitaine 2014 –IR60309-00003281.

Acknowledgment. We thank Simon Lugan, Gil Mery and Thomas Salomon for technical help and also the technological center Alphanov, for technical discussions.

References

1. D. Y. Shen, J. K. Sahu and W. A. Clarkson, Opt. Express 13, 4916-4921 (2005).
2. R. Royon, J. Lhermite, L. Sarger and E. Cormier, Opt. Express 21, 13818-13823 (2013).
3. R. Flaminio, Technical Digest (CD) (Optical Society of America, 2005), paper JTuB4.
4. Y. Jeong, J. Nilsson, J. K Sahu, D. N. Payne, R. Horley, L. M. B.Hickey, & P. W. Turner, IEEE Journal of Selected Topics in Quantum Elect., 13, 546-551. (2007).
5. J. Boullet, G. Guiraud, G. Santarelli, C. Vincont, S. Salort, Proc. SPIE 9730, Components and Packaging for Laser Systems II, 97300Q (March 7, 2016); doi:10.1117/12.2209496.
6. A. Yeniay, J. Delavaux, and J. Toulouse, J. Lightwave Technol. 20, 1425-(2002).
7. M. Fleyer, S. Heerschap, G. A. Cranch, and M. Horowitz, Opt. Lett. 41, 1265-1268 (2016).
8. A. Liem, J. Limpert, H. Zellmer, and A. Tünnermann, Opt. Lett. 28, 1537-1539 (2003).
9. C. Li, S. Xu, X. Huang, Y. Xiao, Z. Feng, C. Yang, K. Zhou, W. Lin, J. Gan, and Z. Yang, Opt. Lett. 40, 1964-1967 (2015).
10. S. Novak and A. Moesle, J. Lightwave Technol. 20, 975- (2002).
11. H. Tünnermann, J. Neumann, D. Kracht, and P. Weßels, Opt. Express 20, 13539-13550 (2012).
12. J. Zhou, J. Chen, Y. Jaouen, L. Yi, X. Li, H. Petit and P. Gallion, IEEE Photonics Technology Letters, 19, 978-980, (2007).
13. M. N. Zervas and C. A. Codemard, IEEE J. Sel. Topics Quantum Electron., vol. 20, no. 5, 2014.
14. L. Zhang, S. Cui, Chi L, J Zhou, and Y. Feng, Opt. Express 21, 5456-5462 (2013).
15. C. Zeringue, C. Vergien, and I. Dajani, Opt. Lett. 36, 618-620 (2011).
16. M. Horowitz, A. R. Chraplyvy, R. W. Tkach and J. L. Zyskind, IEEE Photonics Technology Letters, vol. 9, no. 1, pp. 124-126, Jan. 1997